Centrifuge modeling of failure patterns in mixed soil layers induced by normal faults

La modélisation au centrifuge des allures de déformation au sol des couches mélangées de sol induites par la faille normale

P. Hu[+], Q.P. Cai[++], G.Y. Luo[++], Y.H. Ding[+], M. Dong[++], L.W. Hu[++], Y.J. Hou[++] and C.W.W. Ng[++]

[+]*Beijing Seismological Bureau, Beijing, China*
[++]*Hong Kong University of Science and Technology, HKSAR*

ABSTRACT

Ground failures and ruptures may be induced by fault movements during an earthquake. Numerous notorious earthquakes including the recent Wenchuan earthquake have revealed that surface fault ruptures cause serious damage to structures located near bedrock fault zones. Physical model tests have been conducted by various researchers to investigate the influence of fault movements at one gravity (1-g) and elevated gravity. Most of these physical model tests have been carried out on clear dry sands even though very complex ground failure patterns have been observed in field case studies. In this study, three centrifuge model tests at 120-g were conducted to observe ground failure patterns in different types of soil. Three different models, a sand model, a silt model and a model with mixed soil layers, were tested in the centrifuge. A newly developed hydraulic setup was used at the bottom of the centrifuge models to simulate normal bedrock fault movement with a dip slip angle of 70^o with respect to the horizontal direction. The centrifuge setup, model preparation and testing procedures and experimental results are described, reported and discussed in this paper.

RÉSUMÉ

Des ruptures au sol peuvent être induits par des mouvements de faille pendant un tremblement de terre. Les tremblements de terre notoires nombreux comprenant le tremblement de terre récent de Wenchuan ont indiqué que des ruptures au sol pourraient causer des sérieux dommage aux bâtiments, aux structures et aux services ont placé près des zones faillées potentielles. Bien que des essais sur modèles physiques aient été effectués par de divers chercheurs pour étudier l'influence des mouvements de faille à une gravité (1-g) et à une gravité élevée, la plupart de ces essais ont été effectuées sur les sables secs, qui ne peuvent pas refléter des conditions naturelles exactement. Dans cette étude, trois essais sur modèle au centrifuge à 120 g ont été effectués pour observer les allures des ruptures au sol dans différents types de sol. Un modèle de sable, un modèle de limon et un modèle avec des couches mélangées de sol ont été examinés dans la centrifugeuse. Une installation hydraulique developpée récemment a été employée pour simuler le mouvement de faille normale avec un angle de pendage de 70 o. L'installation de centrifugeuse, la préparation de modèle, les procédures d'essais et les résultats expérimentaux sont décrits, rapportés et discutés en cet article.

Keywords: ground failure patterns, mixed layer soil, normal bedrock fault, centrifuge modeling

1 INTRODUCTION

A large number of notorious earthquakes, such as the Kobe earthquake in 1995 and the Jiji earthquake in 1999, revealed that ground surface fault ruptures cause serious damage to structures located near bedrock fault zones. Recently, the 2008 Wenchuan earthquake (Mw 8.0) induced a major Yingxiu-Beichuan surface fault, stretching more than 180 km (Li et al. 2008), and resulted in the deaths of thousands of people and huge economic losses in China. The dangers of ground surface failures in earthquakes have long been recognized.

To understand the damage to buildings and other public structures caused by surface fault ruptures, many researchers have used different methods to investigate the failure pattern of rupture propagation in the soil alluvium. One-g small-scale physical testing is one method that has been widely utilized (e.g., Cole & Lade 1984, Lade & Cole 1984). These studies focus on determining the location of the surface fault rupture and the width of the affected zone in the alluvium over dip-slip faults. Obviously, the lower stress state compared to the prototype is inherently a limitation of 1-g small-scale physical modeling. Other researchers have used centrifuge to study the mechanisms of fault rupture (e.g., Stone & Wood 1992, Anastasopoulos et al. 2007). By using clear dry sand to model the alluvium, the mechanism of fault rupture propagation, location of the influence zone and the height of the scarp fault on the ground surface was investigated at elevated gravity in these studies.

As geotechnical centrifuge is an excellent physical modeling tool for investigating the mechanism of fault rupture propagation, a single homogeneous soil model has often been tested. Relatively, mixed soil layers are less investigated and reported. In this paper, three centrifuge models: a sand model, a silt model and a model with mixed soil layers, are described and reported. The objectives of the tests are as follows:

a). Investigate the failure patterns on ground surfaces induced by normal fault movements in layered silt-sand profiles.

b). Compare the failure mechanisms and patterns from mixed soil layers with those by homogeneous sand and silt.

2 TEST PROGRAM

The experimental program was designed to evaluate the systematic influence of ground profiles on surface failures induced by normal fault movements. Three centrifuge tests were performed. The first one (T1) was a homogenous sand model test. The second test (T2) was on homogenous silt. In the third test (T3), the model ground profile consisted of mixed layers of sand and silt. The ground profile in T3 was a simplification of a typical ground profile in Beijing, China. All soil samples used in the tests were natural materials obtained from Beijing.

Based on historical earthquakes in China (Guo & Ma 1988), the maximum vertical movement of the bedrock fault is about

Proceedings of the 17th International Conference on Soil Mechanics and Geotechnical Engineering
M. Hamza et al. (Eds.)

doi:10.3233/978-1-60750-031-5-594

0.6 m at a particular location with an earthquake intensity of VIII. To investigate the surface failure at a location with an earthquake intensity of VIII, a vertical bedrock fault movement of about 0.6 m was therefore used in each test. Some basic parameters of each test are summarized in Table 1.

Table 1 The basic parameters of the three centrifuge experiments

Test identity	T1	T2	T3
Soil type	Sand	Silt	Mixed layers of sand and silt
Model height in prototype after consolidation (m)	69.38	63.78	66.63
Dip slip angel of fault with respect to horizontal (°)	70	68	69
Vertical bedrock fault movement in prototype (m)	0.65	0.66	0.67

3 PREPARATION OF MODEL SOILS

Both of the sand and silt utilized in this study were obtained from the Chang Ping area, which is in northern Beijing.

Each type of soil was pretreated before being used. The sandy soil was first air-dried to a water content of about 2.5%. Tap water was then added and mixed thoroughly with the dried sand to a targeted water content of 5.5%. Thereafter, the well-mixed wet sandy sample was kept inside an impervious container for at least 24 h for moisture equalization.

A similar process was applied to the silt sample. However, crushing the agglomerate silt into finer powder was necessary after air-drying. The silt was first crushed by a mixer for about 20 minutes per 50 kg and then passed through a sieve (2 mm × 2 mm) so that there were no uncrushed particles. The targeted water content of the silt sample was 20%. This water content is lower than the plastic limit (PL=22%) of the silt. The relevant sand and silt properties obtained from the laboratory tests are summarized in Table 2.

Table 2 Soil parameters

Soil	D_{50} (mm)	Water content (%)	Plastic Limit (%)	Liquid Limit (%)	ϕ'_{crit} (°)
Sand	0.77	5.5	-	-	37
Silt	0.032	20	22	31	33

4 THE CENTRIFUGE FACILITY AND MODEL CONFIGURATION

The centrifuge tests were conducted in a geotechnical beam centrifuge at the Hong Kong University of Science and Technology (Ng et al. 2004). This centrifuge has a rotating arm with a 4.2 m nominal radius, and a maximum capacity of 400 g-ton. The instrument is able to elevate the model's gravity field up to 150 times for static model tests. The model box that was used is shown in Figures 1(a) and (b). It was an aluminum plane-strain container fitted with a 0.1 m thick Perspex window, which allows observation of the soil during testing. The internal dimension of this strong box was 0.350 m × 1.244 m × 0.851 m (width × length × height).

A new test setup was installed at the bottom of the strong box to simulate the bedrock fault system, as shown in Figure 1(c). The left part of this setup was a base block, bolted to the bottom of the strong box. It was kept stationary during the test to simulate a foot wall. The height of this base block was 0.231 m to permit enough space for bedrock fault simulation. Its length was 0.788 m.

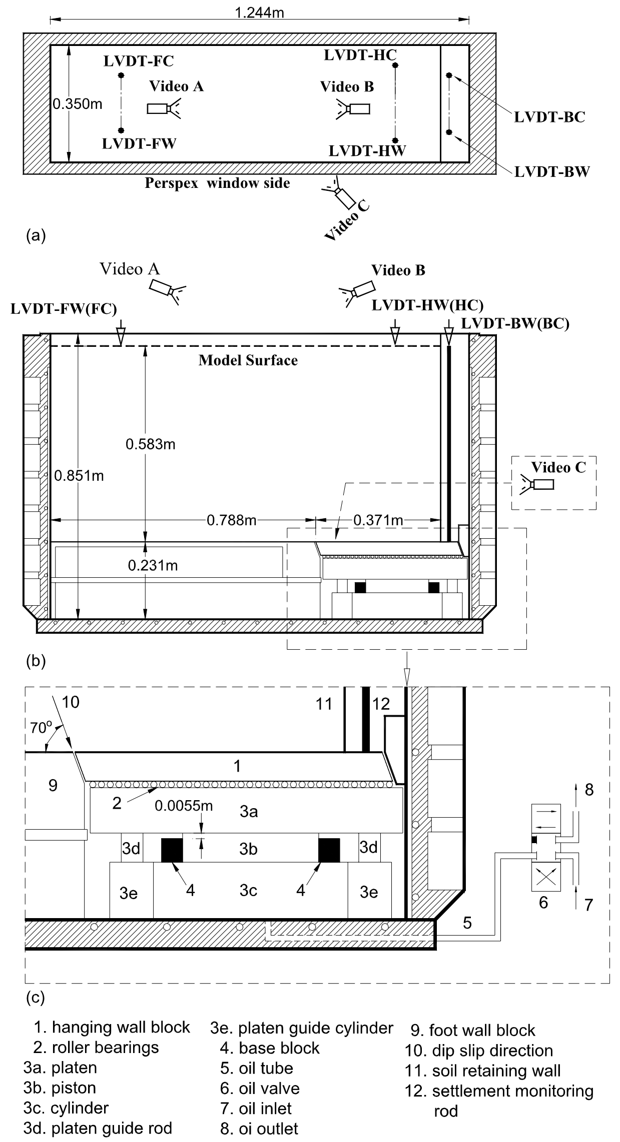

Figure 1. The model package: (a) plan view; (b) sectional view; (c) bedrock fault system.

The right part of test setup, aiming to simulate a hanging wall, mainly consisted of a hanging wall block, a roller bearing system and a hydraulic system. The hanging wall block rested upon the roller bearings, supported by a hydraulic actuator. Driven by this hydraulic actuator, the hanging wall block could move along a preset direction at an angle of 70° with respect to the horizontal direction. The maximum stroke of this hydraulic actuator was about 42 mm.

This test setup was designed to model both normal and reverse bedrock fault movement. However, only normal fault movement was considered in this study. In advance of the model preparation, the piston of the hydraulic actuator was elevated to its maximum capacity with high-pressure (10,000 kPa) oil to ensure that the top of the foot wall block and the hanging wall block were kept at the same height before normal fault simulation. Furthermore, the high pressure oil in the hydraulic system maintained the weight of the overlying soil under both normal gravity and elevated gravity.

Each soil model was constructed by the moist tamping method. Each compaction layer was about 15 mm high. To reduce the non-homogeneity between the compaction layers, the surface of each compaction layer was scratched before compaction of the following layer. The densities of the sand model in T1 and the silt model in T2 were controlled to be 1690 kg/m^3 and 1920 kg/m^3, respectively. Each sand and silt layer in T3 was controlled to have the same density as that in test T1 and T2, respectively.

Figure 2 shows the mixed-layer model in T3. The model consisted of nine soil layers. In each test, the dimensions of the soil model were 0.350 m × 1.159 mm × 0.583 mm (width × length × height) before model consolidation in fight. The distance of the bedrock fault to the left end and the right end of model was 0.788 mm and 0.371 mm, respectively.

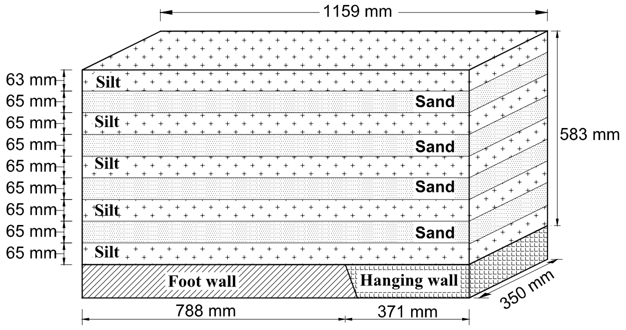

Figure 2. Schematic diagram of the mixed layers in T3.

5 INSTRUMENTATION AND TEST PROCEDURES

After model preparations, the strong box was transferred to the centrifuge. The instrumentation layout for all three tests is presented in Figure 1(a) and (b). All six linearly variable differential transformers (LVDT) and three digital video recorders were used during tests. LVDT-FW and LVDT-FC were mounted on the model surface at the foot wall to record the surface settlement. LVDT-HW and LVDT-HC were mounted on model surface at the hanging wall. LVDT-BW and LVDT-BC were mounted upon two monitoring rods, screwed onto the hanging wall block. The three digital video recorders were used to monitor the model surface failure and bedrock fault movement.

Each test was carried out under a centrifugal acceleration of 120g. After consolidation, normal fault movement was simulated by settlement of the hanging wall block. It was controlled by opening the oil valve. When the oil was drained into a cylinder, the platen fell and then rested upon the adjustable base block, as shown in Figure 1(c). The spacing between the platen and the base block was 0.0055 m in each test. The vertical settlement of the platen was guided by four platen guides around the cylinder. It took about 0.07 s in model time for the hanging wall to finish its movement along the preset direction. The sampling rate was increased to 100 Hz during this process.

After the centrifuge finished spinning, the post experiment observations were made. The differential settlements along the length direction of the models were measured and the failure patterns of the model surfaces were observed. The width and depth of the cracks on the model surface were measured.

6 OBSERVATIONS AND EXPERIMENTAL RESULTS

The experimental results were analyzed to distinguish ground surface failures in different types of soils. Data presented here are converted into prototype, unless stated otherwise. The scaling between the model and the prototype was 1/N (the centrifuge acceleration equaled 120 in this study) for the duration of the bedrock fault movement and 1 for the velocity.

6.1 *Displacement monitoring results*

During the bedrock fault movement, the model surface displacements and bedrock fault movements were recorded by LVDTs. Figure 3 shows the recorded displacements. Because the model was simplified as a two-dimensional one, settlement results were calculated from the average readings of the LVDTs at the same cross section. For example, the model surface settlement at the footwall was calculated by the average of LVDT-FC and LVDT-FW. The moment that the bedrock fault movement happened was set to be the origin of the ordinate.

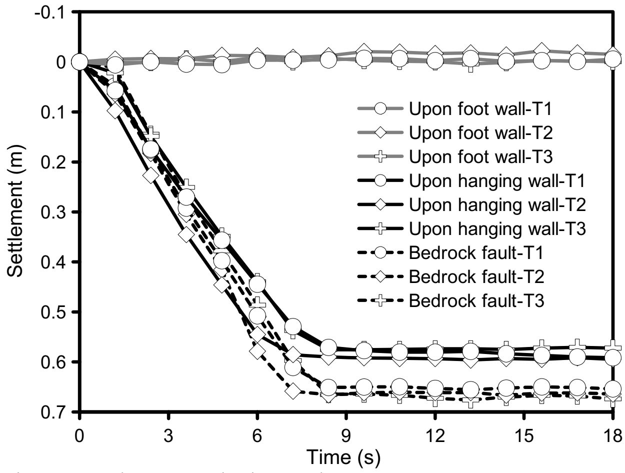

Figure 3. Settlement monitoring results.

It can be seen from the figure that the bedrock fault settlement of about 0.66 m finished within 9 s. The velocity of the bedrock fault movement was about 0.073 m/s. During the movement of bedrock fault, the soil resting on the hanging wall moved at a similar velocity. The settlement of the model surface on the hanging wall was about 90% of the bedrock fault movement in each test. No obvious movement in the soil resting on the foot wall was observed. This different responses of the overlying soil alluvium on the hanging wall and the foot wall suggests that a differential settlement zone on the ground surface developed.

The displacement monitoring results show that differential settlement of the ground surface may be induced by normal bedrock fault movement in sand, silt and mixed-layer soil. The differential settlement on the ground surface appears to be smaller than that in the bedrock fault.

6.2 *Observations on the model surface*

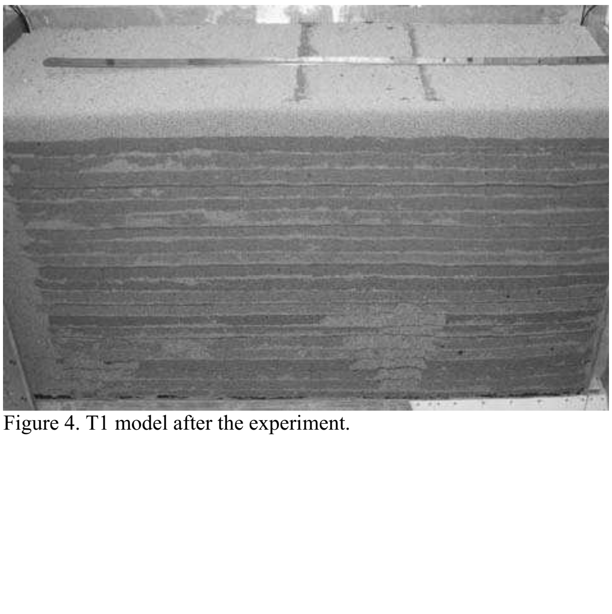

Figure 4. T1 model after the experiment.

The deformed model surfaces were further examined after the centrifuge tests. As shown in Figure 4, no distinct fault scarp can be observed on the model surface in T1. This may be due to the small magnitude of the bedrock fault movement, h, compared to the height of the soil model, H. The value of h/H equaled 0.94% in this test. Compared to Anastasopoulos's results in dry sandy soil (Anastasopoulos et al. 2007), the value of h/H in this test is smaller than the 1% required for the bedrock fault to propagate up to the ground surface. Water in the sand model in this test may be another reason for the absence of scarp faults on the model surface.

Figure 5(a) shows the three cracks observed on the model surface in T2. These cracks covered a zone about 26 m in width, located near the intersection of the bedrock fault plane and the model surface. The major crack was the middle one, with a width of 0.26 m and a depth about 4.2 m. As described by Bray (1994), a similar ground failure pattern was observed in the 1983 Borah Peak earthquake. They observed that 'tension cracks with little vertical displacement formed at the point of maximum flexure, instead of fault scarp when the alluvium was wet, fine-grained sediments'. All these results suggest that ground surface failures may not necessarily propagate from the bedrock fault. Ground surface cracks may be produced even when the vertical settlement of the bedrock fault is small.

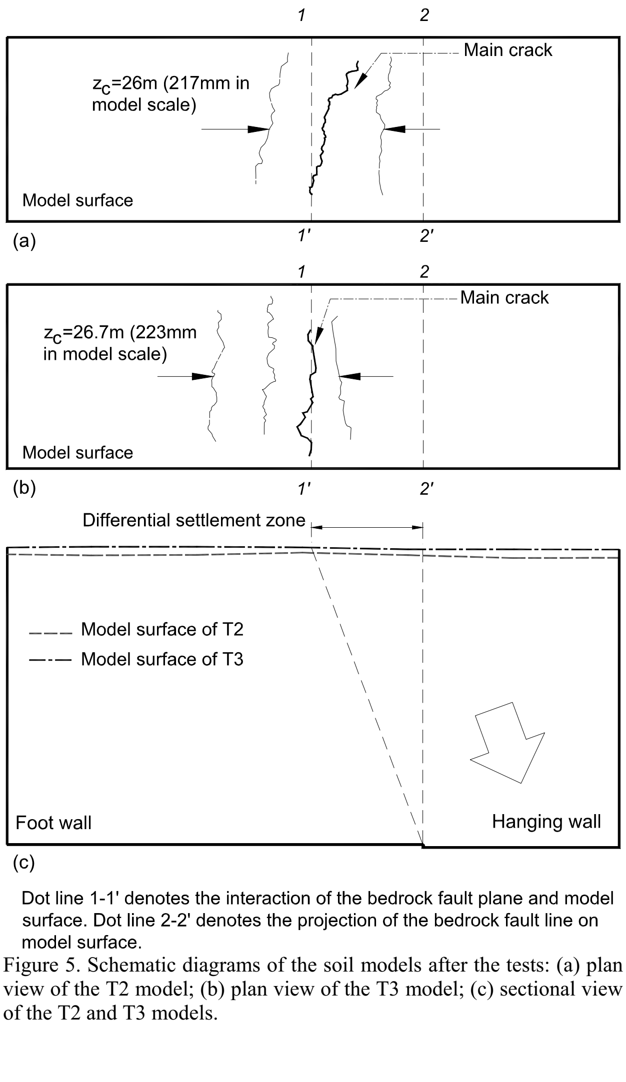

Figure 5. Schematic diagrams of the soil models after the tests: (a) plan view of the T2 model; (b) plan view of the T3 model; (c) sectional view of the T2 and T3 models.

Similar ground surface cracks can be observed on the surface of the T3 test after the bedrock fault movement, as shown in Figure 5 (b). The width of the influencing zone of these cracks was about 26.7 m. The major surface crack in this test was found to be located near the intersection line 1-1', with a width of about 0.22 m. This result demonstrates that ground surface failures do not have to develop from the bedrock fault. This main ground surface crack passed through the whole top silt layer. However, in the following sandy layer, no obvious crack could be observed. Development of cracks on the model surface may cease when they reach sand.

Measurements of the ground settlement on the model surfaces in T2 and T3 after spinning down the centrifuge are given in Figure 5(c). These results confirm the differential settlement zone that may be induced by normal fault movement.

7 CONCLUSIONS

Ground surface failures in different types of soil profile induced by normal fault movement were investigate in a series of centrifuge tests. Based on these tests, the following main conclusions may be drawn:

a). Differential settlement of the ground surface is one of the surface failure patterns that can be induced by normal bedrock fault movements in sandy, silty or mixed-layer soil. Vertical differential settlement of the ground surface is smaller than that observed in the bedrock fault.

b). Surface cracks are a typical failure pattern that can be induced by normal fault movements in silty soil. Different from the scarp fault that may happen in sandy soil, a ground surface crack does not originate and propagate from the bedrock fault. On the contrary, crack starts from ground surface and propagates into the soil.

c). Ground surface cracks can also be observed in mixed layers when the top layer is silty soil. It is found that development of crack failure may cease once the crack reaches sand.

ACKNOWLEDGMENT

The authors would like to thank Dr A.C.F. Chiu for his assistance in translating the paper title and abstract into French.

REFERENCES

Anastasopoulos, I. Gazetas, G., Bransby, M. F., Davies, M. C. R. and Nahas, E. A. 2007. Fault rupture propagation through sand: finite-element analysis and validation through centrifuge experiments, Journal of Geotechnical and Geoenvironmental Engineering, ASCE, Vol.133, No.8, pp.943-958.

Cole, D. A. and Lade, P. V. 1984. Influence zones in alluvium over dip-slip faults, Journal of Geotechnical Engineering, ASCE, Vol.110, No.5, pp.599-615.

Guo, J. Z. and Ma, Z. J. 1988. Research on great earthquakes in China, Beijing, Seismological Press.

Lazarte, C. A. and Bray, J. D. 1996. A study of strike-slip faulting using small scale models, Geotechnical Testing Journal, Vol.19, No.2, pp.118-129.

Lade, P. V., Cole Jr D. A. and Cummings, D. 1984. Multiple failure surfaces over dip-slip faults, Journal of Geotechnical Engineering, ASCE, Vol.110, No.5, 616-627.

Li, Y., Zhou, R. J., Dong, S. L., Zhang, Y., He, Y. L., Chen, H., Yan, L., Qiao, B. C. and Ma, B. L. 2008. Surface rupture, thrusting and strike-slipping in Wenchuan earthquake of Sichuan, China, Journal of Chengdu University of Technology, Vol.35, No.4, 404-413.

Ng, C. W. W., Li, X. S., Van Laak, P.A. and Hou, Y. J. 2004. Centrifuge modeling of loose fill embankment subjected to uni-axial and bi-axial earthquake, Soil Dynamics and Earthquake Engineering, Vol.24, No.4, pp.305-318.

Stone, K. J. L. and Wood, D. M. 1992. Effects of dilatancy and particle size observed in model tests on sand, Soils and foundations, Vol.32 No.4, 43-57.